

Supporting Information

Potential Detection of Cancer with Fluorinated Silicon Nanoparticles in ^{19}F MR and Fluorescence Imaging

Sha Li^a, Yaping Yuan^a, Yuqi Yang^a, Conggang Li^a, Michael T. McMahon^{b,c}, Maili Liu^a, Shizhen Chen^{*a} and Xin Zhou^{*a}

^a Key Laboratory of Magnetic Resonance in Biological Systems, State Key Laboratory of Magnetic Resonance and Atomic and Molecular Physics, National Center for Magnetic Resonance in Wuhan, Wuhan Institute of Physics and Mathematics, Chinese Academy of Sciences, Wuhan 430071, China

*E-mail: chenshizhen@wipm.ac.cn, xinzhou@wipm.ac.cn

^b Russell H. Morgan Department of Radiology and Radiological Science, The Johns Hopkins University School of Medicine, Baltimore, Maryland 21287, United States

^c F.M. Kirby Research Center for Functional Brain Imaging, Kennedy Krieger Institute, Baltimore, Maryland 21287, United States

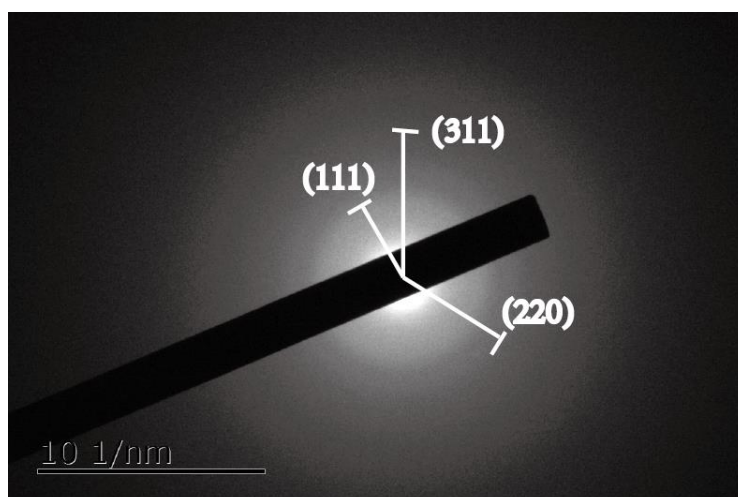


Figure S1 Selected area electron diffraction pattern (SAED) of $^{19}\text{FSiNPs}$. The SAED pattern for $^{19}\text{FSiNPs}$ can be indexed to the [111], [220] and [311] diffraction rings and is in good agreement with the face-centered cubic structure.

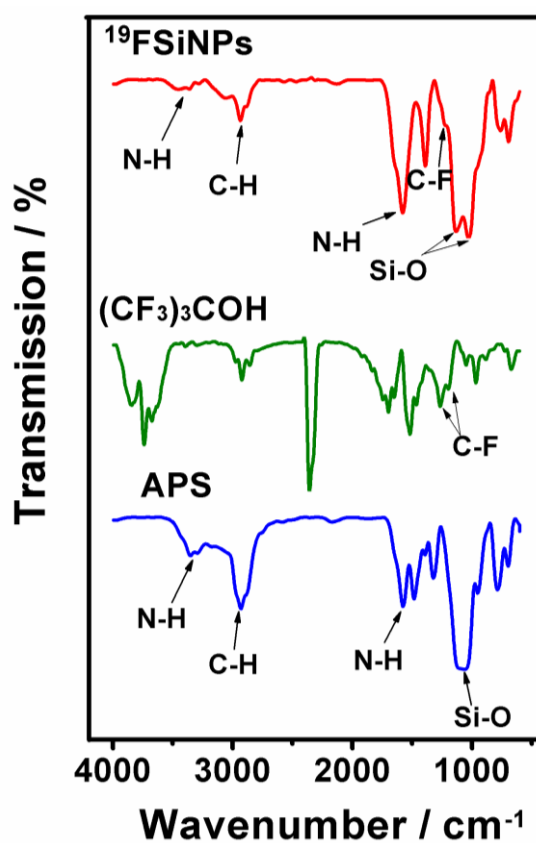


Figure S2 FTIR spectral of $^{19}\text{FSiNPs}$ (red line), $(\text{CF}_3)_3\text{C-OH}$ (green line), APS (blue line).

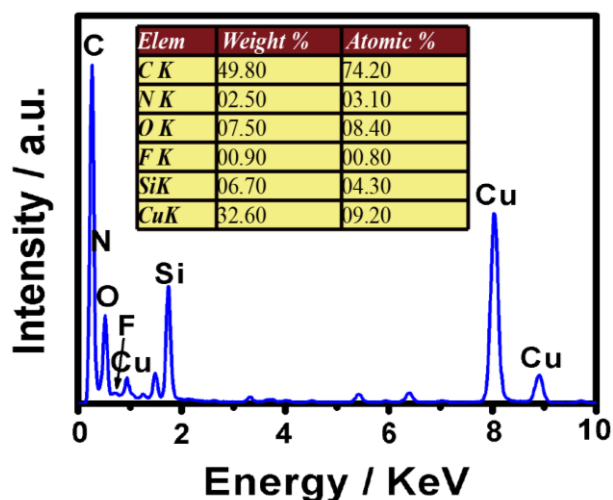


Figure S3 A typical EDX pattern of the prepared $^{19}\text{FSiNPs}$. Inset table presents the corresponding elemental ratios (weight and atom percentage) calculated by the EDX software (K-shell intensity ratios are indicated). The EDX pattern qualitatively demonstrates the existence of Si and O in the SiNPs.

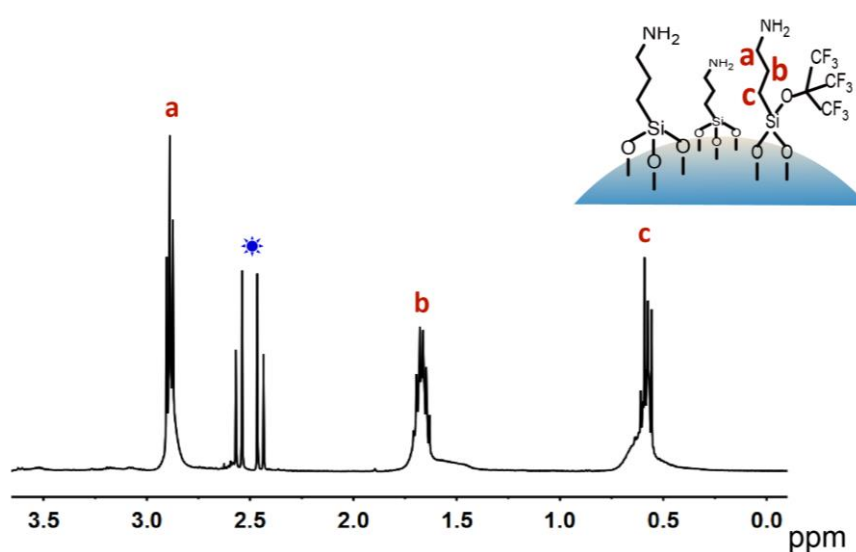


Figure S4 The ^1H NMR spectra of $^{19}\text{FSiNPs}$. Residual ethoxy group ($-\text{CH}_2-$) protons of trisodium citrate dihydrate mixed with $^{19}\text{FSiNPs}$ are denoted by (\star).

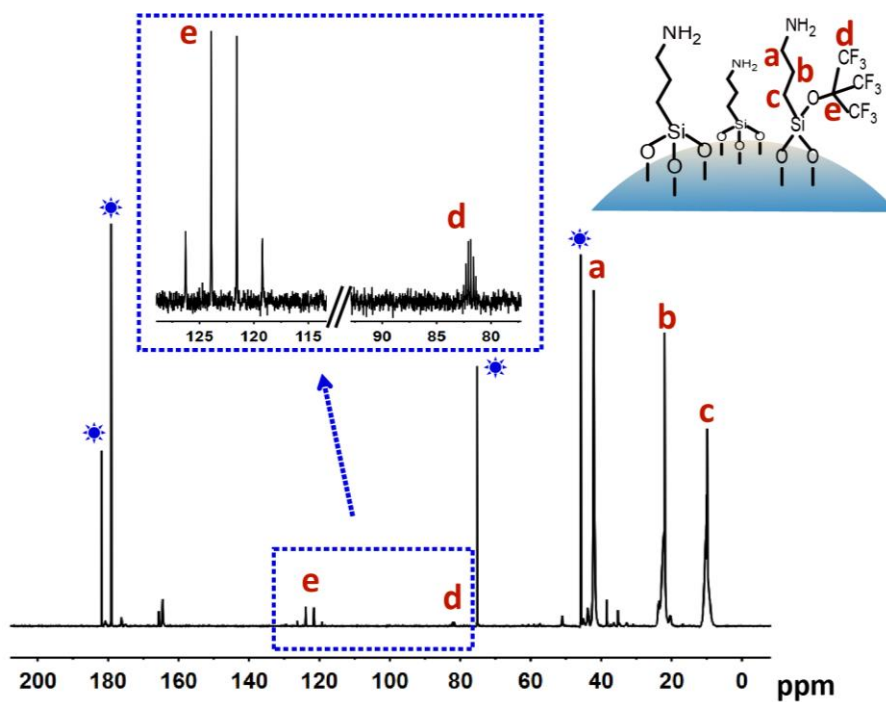


Figure S5 The ^{13}C NMR spectra of $^{19}\text{FSiNPs}$. Residual carbon signal of trisodium citrate dihydrate mixed with $^{19}\text{FSiNPs}$ are denoted by (\odot).

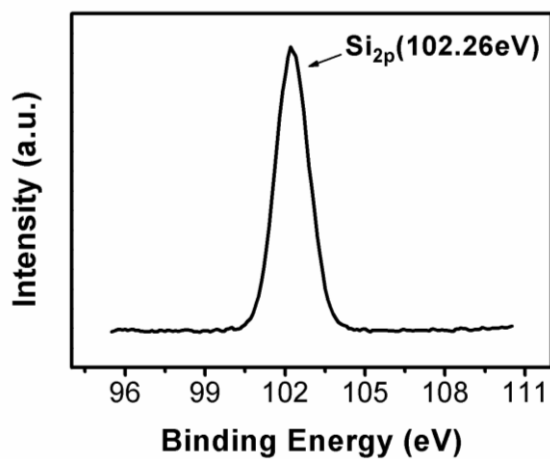


Figure S6 High-resolution XPS spectra of silicon (2p)

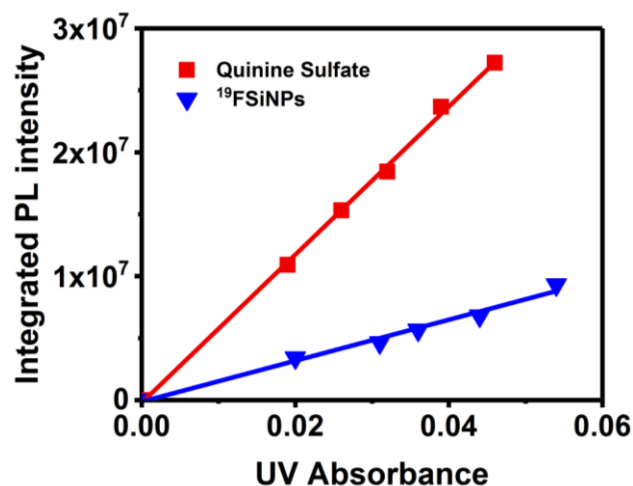


Figure S7 Photoluminescence quantum yield (PLQY) measurements of ¹⁹FSiNPs. PLQY determination of ¹⁹FSiNPs was relative calculated vs. a standard whose quantum efficiency has been accurately determined.^[1] Quinine sulfate in 0.1 M H₂SO₄ (literature quantum yield: 58%) was chosen as the reference and freshly prepared to reduce the measurement error.^[2] Quantum yield can be calculated using the expression: $Q_s = Q_r (K_s/K_r) (\eta_s/\eta_r)^2$, Here the indices s and r, respectively, denote sample and reference. Where Q is the QY, K is the slope determined by the curves and η is the refractive index of the solution. The integrated PL intensity of ¹⁹FSiNPs was dependence on the UV absorbance and the PLQY was calculated to be 16.1%.

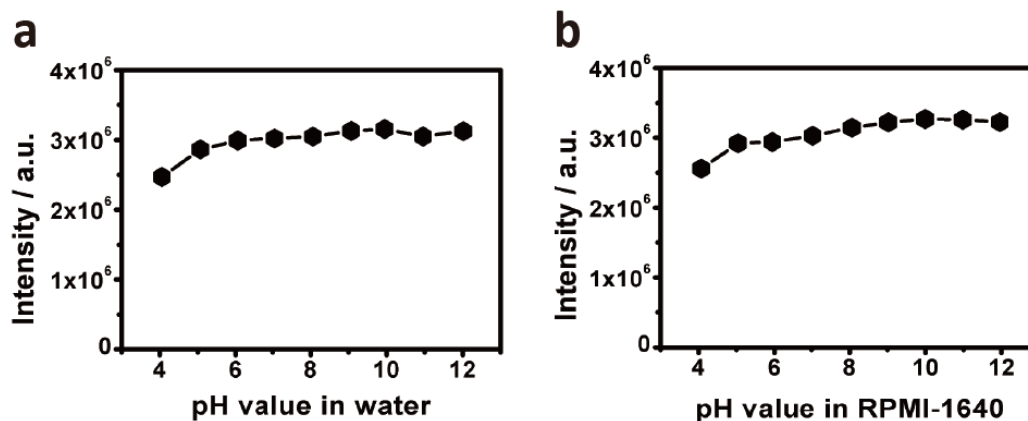


Figure S8 Temporal evolution of fluorescence intensity of ¹⁹FSiNPs in (a) water and (b) RPMI-1640 medium under various pH values. ¹⁹FSiNPs maintain strong PL in the wide pH range of 4-12 in water and RPMI-1640 medium.

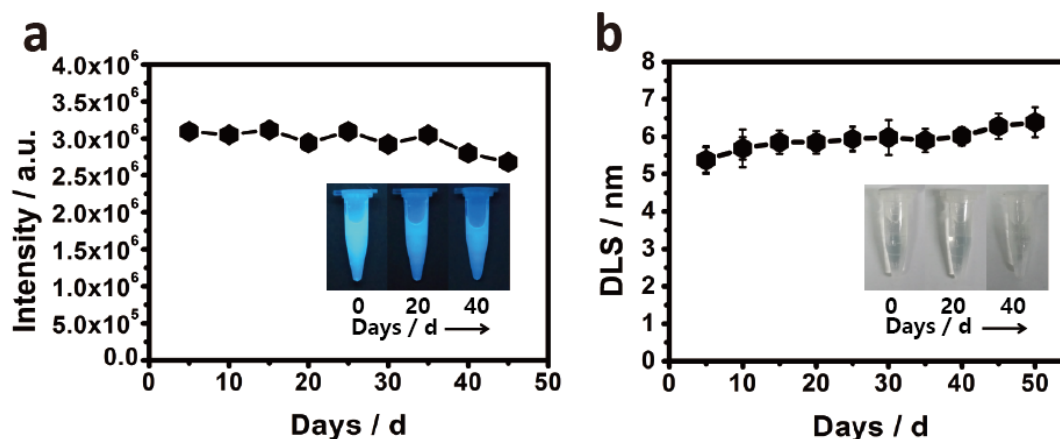


Figure S9 The storage stability of ¹⁹FSiNPs. (a) PL intensity and (b) DLS values of the ¹⁹FSiNPs dispersed in water for different time intervals. The results showed that the as-prepared ¹⁹FSiNPs exhibit about 13% loss of PL intensity after 45 days storage. DLS confirmed that the ¹⁹FSiNPs get slightly aggregation among the 50 days storage as the hydrodynamic diameter increase slightly from 5.37 nm to 6.38 nm.

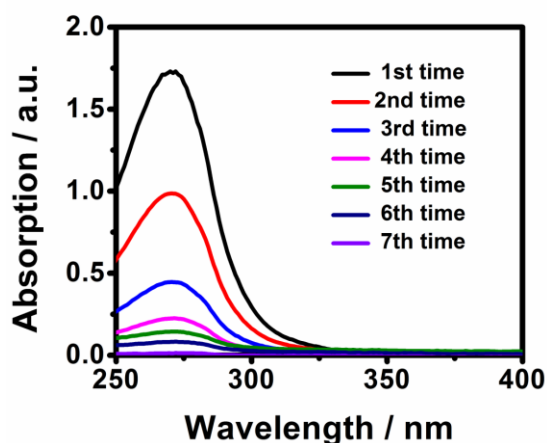


Figure S10 The UV-vis absorbance spectra of the ¹⁹FSiNPs-RGD filtered solutions after purification using 3 kDa Millipore ultra-filtration tubes through centrifugation (6500 rpm × 15 min, per time). Obviously, the absorbance at 275 nm was close to zero after ultrafiltration for seven times, indicating adequate removal of unreacted c(RGDyC) peptides.

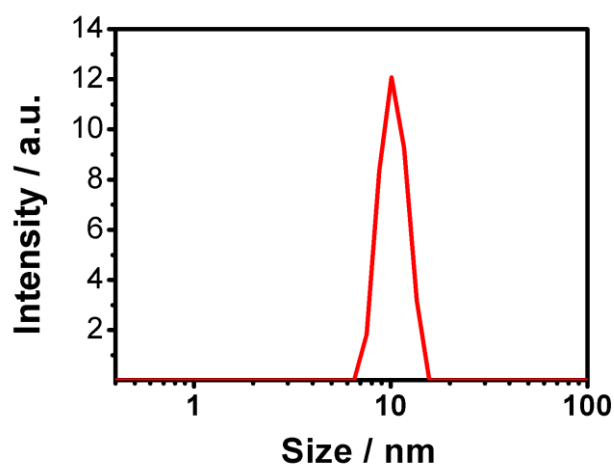


Figure S11 DLS measurement of $^{19}\text{FSiNPs-RGD}$ in water. The hydrodynamic diameter (10 nm) of $^{19}\text{FSiNPs-RGD}$ is obviously larger than that measured of $^{19}\text{FSiNPs}$ (5.37 nm).

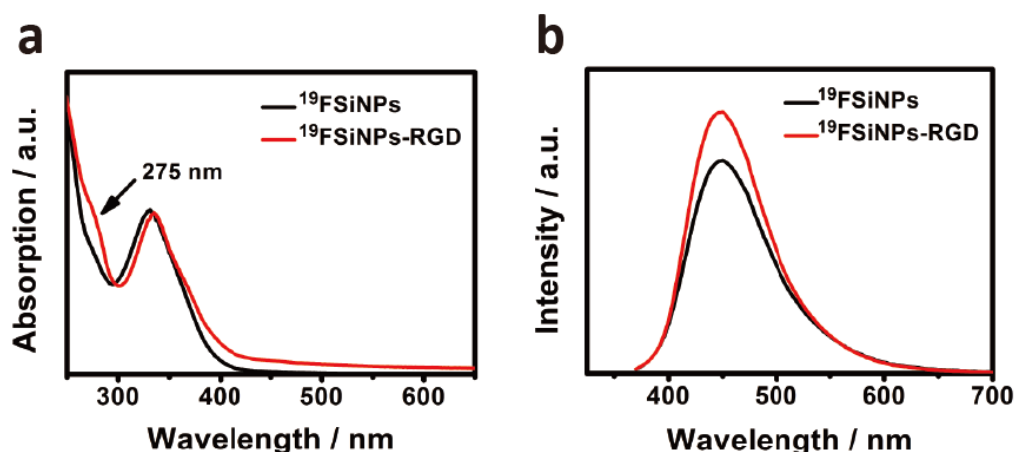


Figure S12 (a) UV and (b) PL spectra of $^{19}\text{FSiNPs}$ (black lines) and $^{19}\text{FSiNPs-RGD}$ (red lines). Both the prepared $^{19}\text{FSiNPs}$ and the $^{19}\text{FSiNPs-RGD}$ show similar absorption and photoluminescence spectra. Notably, the solution of $^{19}\text{FSiNPs-RGD}$ exhibit an extra absorption at 275 nm which is ascribed to RGD compared to pure $^{19}\text{FSiNPs}$, indicating the successful conjugation of $^{19}\text{FSiNPs}$ and RGD peptide. In addition, the $^{19}\text{FSiNPs-RGD}$ exhibit much stronger fluorescence. According to the previous research,^[2] it is RGD peptide containing aromatic electron-rich systems capped outside the nanoparticle that facilitate effective suppression of nonradiative decay processes and emissive recombination channel across the entire SiNPs.

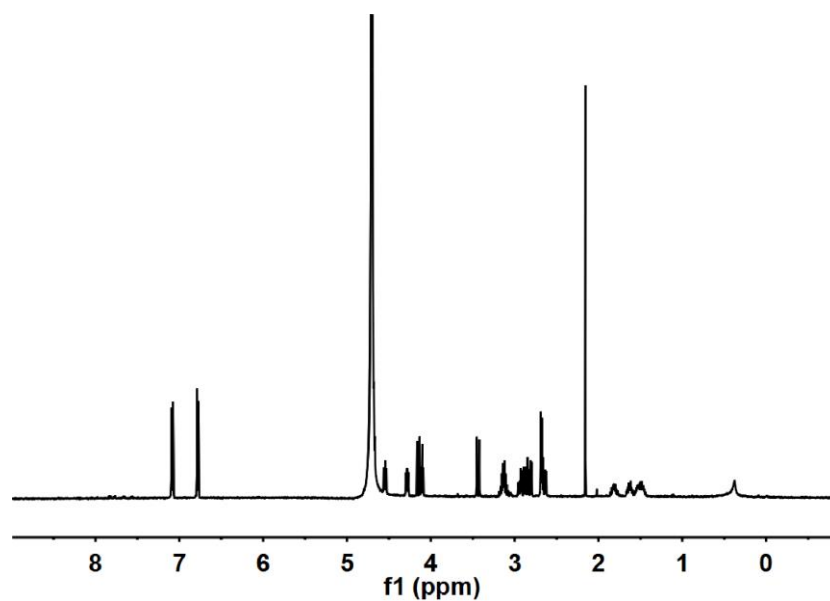


Figure S13 The ¹H NMR spectra of cyclic RGD-containing peptides in D₂O

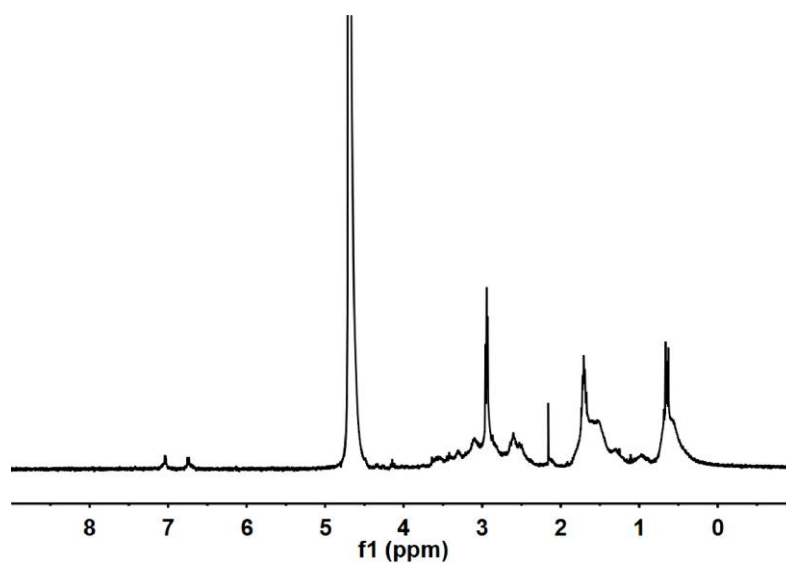


Figure S14 The ¹H NMR spectra of ¹⁹FsiQDs-RGD in D₂O

Compared to ¹H-NMR of ¹⁹FsiNPs, the signal peak at around ~7 ppm attributed to the RGD-associated aromatic proton was detected in ¹⁹FsiNPs-RGD sample, demonstrating the existence of RGD on the ¹⁹FsiNPs.

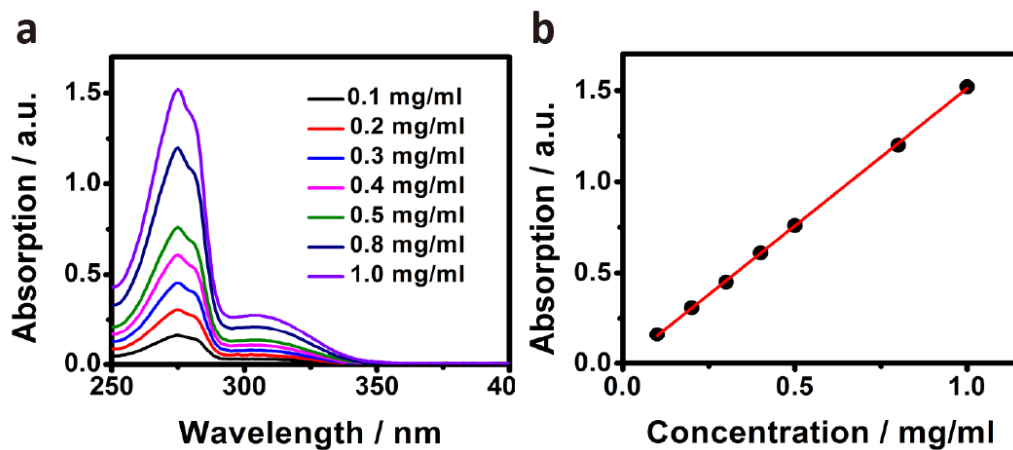


Figure S15 (a) The UV-vis absorbance spectra of c(RGDyC) peptides with different concentrations. (b) Calibration curve of absorbance at 275 nm versus concentrations. The fitting relation is as follow: $y=1.5058x+0.0058$ ($R^2=0.9992$) where y is the absorbance at 275 nm of c(RGDyC) peptide and x is the concentration.

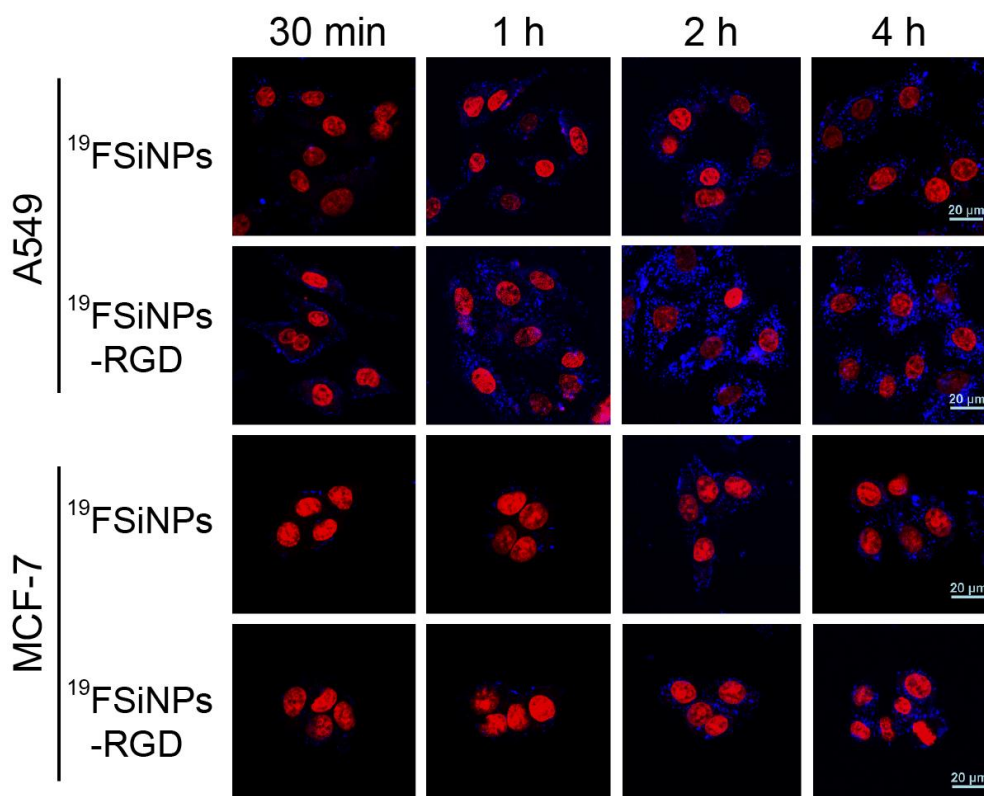


Figure S16 Fluorescence imaging of A549 and MCF-7 cells with pure $^{19}\text{FSiNPs}$ and $^{19}\text{FSiNPs-RGD}$ for specific times captured by laser scanning confocal microscopy. Cells are incubated with nanoparticles (UV absorption of SiNP at 338 nm was set to be 0.1) for specific times at 37 °C followed by treatment with RedDot2 for 30 min. The fluorescence of SiNPs and RedDot2 is defined as blue and red, respectively. The results showed that $^{19}\text{FSiNPs}$ and $^{19}\text{FSiNPs-RGD}$ was gradually swallowed into the cells in a time-dependent manner and accumulated in the cytoplasm. In addition, distinct blue fluorescence signal was visualized in $^{19}\text{FSiNPs-RGD}$ treated A549 cells which is well known of over-expression of $\alpha_v\beta_3$ integrin. These data convincingly confirmed the high affinity and integrin $\alpha_v\beta_3$ -specific binding of $^{19}\text{FSiNPs-RGD}$.

Reference:

- [1] Morris, J. V.; Mahaney, M. A.; Huber, J. R. Fluorescence quantum yield determinations. 9,10-Diphenylanthracene as a reference standard in different solvents. *J. Phys. Chem.* 1976, **80**, 969–974.
- [2] Song, C. X.; Zhong, Y. L.; Jiang, X. X.; Peng, F.; Lu, Y. M.; Ji, X. Y.; Su, Y. Y.; He, Y. Peptide-Conjugated Fluorescent Silicon Nanoparticles Enabling Simultaneous Tracking and Specific Destruction of Cancer Cells. *Anal. Chem.* 2015, **87**, 6718-6723.